Integrated Transmission and Distribution System Expansion Planning Under Uncertainty

Gregorio Muñoz-Delgado, *Member, IEEE*, Javier Contreras, *Fellow, IEEE*, José M. Arroyo, *Fellow, IEEE*, Agustin Sanchez de la Nieta, *Member, IEEE*, and Madeleine Gibescu, *Member, IEEE*

***Abstract*—The increased deployment of distributed generation calls for the coordination and interaction between the transmission and distribution levels. This requirement is particularly relevant for planning purposes when renewable-based generation is involved. Unfortunately, in current industry practice, transmission and distribution network planners solve their problems independent of each other, thereby leading to suboptimal solutions. Within this context, this paper addresses the integrated expansion planning problem of transmission and distribution systems where investments in network and generation assets are jointly considered. Several alternatives are available for the installation of lines as well as conventional and renewable-based generators at both system levels. Thus, the optimal expansion plan identifies the best alternative for the candidate assets under the uncertainty associated with demand and renewable-based power production. The proposed model is an instance of stochastic programming wherein uncertainty is characterized through a set of scenarios that explicitly capture the correlation between the uncertain parameters. The resulting stochastic program is driven by the minimization of the expected total cost, which comprises the costs related to investment decisions and system operation. The associated scenario-based deterministic equivalent is formulated as a mixed-integer linear program for which finite convergence to optimality is guaranteed. Numerical results show the effective performance of the proposed approach.**

***Index Terms*—Distributed generation, integrated transmission and distribution planning, network and generation investment decisions, stochastic programming, uncertainty.**

NOMENCLATURE

The main notation used in the paper is defined in this section. Superscripts "T" and "D" are used to denote the correspondence of sets, parameters, and variables to the transmission and distribution levels, respectively. Additional symbols related to the scenario-generation procedure are defined in Section II.

Indices

a	Index for distribution systems.
b	Index for time blocks.
d	Index for demands.
g	Index for generators.
l	Index for lines.
n	Index for nodes.
p	Index for generator types.
s	Index for short-term uncertainty scenarios.
ω	Index for long-term uncertainty scenarios.

Sets

$\mathcal{A}$	Index set of distribution systems.
$\mathcal{B}$	Index set of time blocks.
$\mathcal{D}^D$, $\mathcal{D}^T$	Index sets of demands.
$\mathcal{D}_n^D$, $\mathcal{D}_n^T$	Index sets of demands connected to node n.
$\mathcal{G}_p^D$, $\mathcal{G}_p^T$	Index sets of existing generators.
$\mathcal{G}_p^{D+}$, $\mathcal{G}_p^{T+}$	Index sets of candidate generators.
$\mathcal{G}_{pn}^D$, $\mathcal{G}_{pn}^T$	Index sets of existing generators connected to node n.
$\mathcal{G}_{pn}^{D+}$, $\mathcal{G}_{pn}^{T+}$	Index sets of candidate generators connected to node n.
$\mathcal{L}^D$, $\mathcal{L}^T$	Index sets of existing lines.
$\mathcal{L}^{D+}$, $\mathcal{L}^{T+}$	Index sets of candidate lines.
$\mathcal{N}^D$, $\mathcal{N}_a^{D+}$, $\mathcal{N}^T$, $\mathcal{N}^\infty$	Index sets of distribution, new distribution, transmission, and interface nodes, respectively, where $\mathcal{N}_a^{D+} \subset \mathcal{N}^D$ and $\mathcal{N}^\infty \subset \mathcal{N}^T$.
$\mathcal{P}^D$, $\mathcal{P}^T$	Sets of generator types. $\mathcal{P}^D = \{C^D, W^D\}$ and $\mathcal{P}^T = \{C^T, W^T\}$, where C and W stand for conventional and renewable-based power generation, respectively.
$\mathcal{S}_b$	Index set of short-term uncertainty scenarios for time block b.
Ω	Index set of long-term uncertainty scenarios.

Parameters

$fr(l)$, $to(l)$	Sending and receiving nodes.
$\overline{IC}$	Annualized investment budget.
$IC_{gp}^{G,D}$, $IC_{gp}^{G,T}$	Annualized investment cost coefficients for generators.
$IC_l^{L,D}$, $IC_l^{L,T}$	Annualized investment cost coefficients for lines.

Manuscript received July 17, 2020; revised November 27, 2020 and March 2, 2021; accepted April 2, 2021. Date of publication April 6, 2021; date of current version August 23, 2021. This work was supported in part by the Ministry of Science, Innovation and Universities of Spain under Project RTI2018-096108-A-I00 and Project RTI2018-098703-B-I00 (MCIU/AEI/FEDER, UE), and in part by the Universidad de Castilla-La Mancha under Grant 2020-GRIN-29009. Paper no. TSG-01106-2020. *(Corresponding author: Javier Contreras.)*

Gregorio Muñoz-Delgado, Javier Contreras, and José M. Arroyo are with the Escuela Técnica Superior de Ingeniería Industrial, Universidad de Castilla-La Mancha, 13071 Ciudad Real, Spain (e-mail: gregorio.munoz@uclm.es; javier.contreras@uclm.es; josemanuel.arroyo@uclm.es).

Agustin Sanchez de la Nieta and Madeleine Gibescu are with the Copernicus Institute of Sustainable Development, Utrecht University, 3584 CB Utrecht, The Netherlands (e-mail: agustinsnl@gmail.com; m.gibescu@uu.nl).

Color versions of one or more figures in this article are available at https://doi.org/10.1109/TSG.2021.3071385.

Digital Object Identifier 10.1109/TSG.2021.3071385

M^D, M^T	Sufficiently large positive constants.
$OC_{gp}^{G,D}$, $OC_{gp}^{G,T}$	Production cost coefficients for generators.
$OC_{d}^{U,D}$, $OC_{d}^{U,T}$	Load-shedding cost coefficients.
$P_{d}^{D,D}$, $P_{d}^{D,T}$	Peak consumption levels.
$\overline{P}_{gp}^{G,T}$, $\overline{S}_{gp}^{G,D}$	Power capacities of generators.
$\overline{P}_{l}^{L,T}$, $\overline{S}_{l}^{L,D}$	Line power flow capacities.
R_l^D	Distribution line resistance.
$\underline{V}^D$, $\overline{V}^D$	Lower and upper limits for distribution nodal voltages.
X_l^D, X_l^T	Line reactances.
$\overline{X}_{gp}^{G,D}$, $\overline{X}_{gp}^{G,T}$	Upper bounds for installed generation.
Δ_{bs}	Number of hours for short-term uncertainty scenario s at time block b.
μ_{nbs}^{L}, μ_{nbs}^{W}	Average factors for demand and renewable-based power production.
μ_{ω}^{LG}	Demand growth factor.
π_ω	Probability of occurrence of long-term uncertainty scenario ω.
ρ_{nb}	Nodal power factor.
Variables	
c^T	Expected total cost.
$c^{I,D}$, $c^{I,T}$	Annualized investment costs.
$c^{O,D}$, $c^{O,T}$	Expected operating costs.
$p_{gpbs\omega}^{G,D}$, $p_{gpbs\omega}^{G,T}$	Active power outputs of generators.
$p_{lbs\omega}^{L,D}$, $p_{lbs\omega}^{L,T}$	Active power flows across lines.
$p_{dbs\omega}^{U,D}$, $p_{dbs\omega}^{U,T}$	Levels of load shedding.
$q_{gpbs\omega}^{G,D}$, $q_{lbs\omega}^{L,D}$	Generation levels and line flows of reactive power.
$v_{nbs\omega}$, $\delta_{nbs\omega}$	Squared magnitude and phase angle of nodal voltages.
$x_{gp}^{G,D}$, $x_{gp}^{G,T}$	Investment variables for generators.
$x_{l}^{L,D}$, $x_{l}^{L,T}$	Binary investment variables for lines.

I. Introduction

TRADITIONALLY, demand has been supplied by large-scale generating units connected to the transmission level, thereby allowing distribution systems to be passively operated. Therefore, transmission and distribution systems have been conventionally operated and planned in a separate way [1]–[3]. A relevant example of such industry practice can be found in Spain, where the set of input data for the transmission network planner includes the investment decisions previously made by the distribution network planners [4], [5]. However, the increasing penetration of distributed energy resources, e.g., distributed generation (DG), in worldwide distribution systems has triggered the need for the coordination and interaction between the transmission and distribution levels [6]. According to ENTSO-E [7], in a planning setting, such interactions require integrated approaches that recognize the growing interdependence of transmission and distribution networks. Thus, planning approaches should jointly consider both system levels to find the most effective and efficient network solution and generation deployment. This requirement is particularly relevant when renewable-based generation is involved [7].

The integrated operation of transmission and distribution systems has been addressed in [8]–[15], among others. These works proposed several coordination schemes where transmission and distribution system operators play different roles. However, to the best of our knowledge, little attention has been paid so far to the joint consideration of transmission and distribution systems within a planning context. Relevant exceptions are [16], focused on distribution network planning, [17], devoted to transmission network planning, and [18]–[21], adopting an integrated planning framework.

In [16], the coordinated expansion planning of several distribution systems was addressed while considering transmission system operation. In [17], a transmission network expansion planning model considering the operation of distribution systems was proposed. Note, however, that integrated planning decisions for both system levels were disregarded in [16] and [17].

In [18], the simultaneous expansion planning of transmission and distribution networks was addressed by a deterministic model and a genetic algorithm.

In [19], a scenario-based stochastic programming framework was proposed to make network investment decisions under demand uncertainty. The planning problem was solved through a decentralized optimization algorithm based on the analytical target cascading.

In [20], network and storage investment decisions were considered at both voltage levels under two scenarios for future generation capacity. To that end, a simulation-based algorithm relying on several heuristic approaches was applied.

In [21], a hybrid robust and stochastic expansion planning model was presented. Investment decisions for network and conventional generation assets were considered. In addition, the fleet of existing generators comprised conventional units and a single wind power plant at the transmission level. The uncertainty in wind power production at the transmission level was incorporated through a robust optimization setting whereas the uncertainty in demand at the distribution level was characterized through a scenario-based stochastic programming framework. The resulting problem was solved by using a modified version of the decentralized method presented in [19].

Unfortunately, investment decisions on conventional generators at both system levels were ignored in [17]–[20] whereas, in [16], investments in generators were solely considered at the distribution level. Moreover, investments in renewable-based generators at both system levels were disregarded in [16]–[21]. It is also worth noting that existing renewable-based generation at both system levels was neglected in [16], [18], [19] and scarcely modeled for the transmission level in [21]. In addition, the long-term uncertainty associated with demand growth was disregarded at both system levels in [16]–[21]. Furthermore, the short-term uncertainty related to the variability of demand was neglected at both system levels in [16] and [18] and only accounted for at the distribution level in [21]. Analogously, the short-term uncertainty due to the variability of renewable-based generation was ignored at both system levels in [16], [18], [19] and only considered at the transmission level in [21]. Note also that an insufficient number of scenarios were used for the uncertain parameters that were modeled in [17], [19], [21].

TABLE I
COMPARISON OF PLANNING MODELS JOINTLY CONSIDERING TRANSMISSION AND DISTRIBUTION SYSTEMS

Approach	Integrated planning	T&D network investment	T&D generation investment		T&D uncertainty modeling		
			Conventional generators	Renewable generators	Demand growth	Demand variability	Renewable generation variability
[16]	×	×(1)	×(1)	×	×	×	×
[17]	×	×(2)	×	×	×	✓	✓
[18]	✓	✓	×	×	×	×	×
[19]	✓	✓	×	×	×	✓	×
[20]	✓	✓	×	×	×	✓	✓
[21]	✓	✓	✓	×	×	×(1)	×(2)
Proposed approach	✓	✓	✓	✓	✓	✓	✓

(1) Only at the distribution level
(2) Only at the transmission level

Motivated by the shortcomings of [16]–[21], in this paper, we propose a novel scenario-based approach relying on stochastic programming [22] for the integrated expansion planning of transmission and distribution systems under uncertainty. The proposed integrated model adopts a coordination scheme whereby a centralized planner is responsible for system-wide investment decisions at both the transmission and distribution levels, as is the case in Northern and Southern China. Such a coordination scheme is analogous to the Transmission-System-Operator-managed category described in [15] for operation. It should be noted that the proposed approach substantially departs from state-of-the-art works [16]–[21] from both the modeling and methodological perspectives. Unlike [16]–[21], investment decisions comprise the installation of both lines and generators, including conventional and renewable-based units, at both system levels. Moreover, as another salient feature over [16], [18], [19], [21], existing generation also comprises conventional and renewable-based generators at both system levels. In contrast to [16], [18], [19], [21], the short-term uncertainty related to the variability of demand and renewable-based power production is accounted for at both system levels by a suitable set of scenarios that are generated using historical data and the technique described in [23]. Thus, the correlation between the sources of short-term uncertainty is properly captured. In addition, the long-term uncertainty related to demand growth neglected in [16]–[21] is also accounted for in the proposed approach. As for network effects, a dc load flow model is used to characterize the transmission network whereas, different from [16]–[21], a linearized ac model is used for the distribution network. As a consequence, the resulting scenario-based deterministic equivalent is formulated as a mixed-integer linear program driven by the minimization of the expected investment and operating costs. The relevance of this distinctive methodological aspect with respect to [16]–[21] is twofold. It is worth emphasizing that, based on the availability of both feasible and relaxed solutions setting bounds for the optimal value of the objective function, existing techniques for mixed-integer linear programming guarantee finite convergence to the optimum while providing a measure of the distance to optimality along the solution process [24]. For a proof of finite convergence to optimality, the interested reader is referred to [24, Proposition 2.1]. Additionally, effective, albeit case-dependent, off-the-shelf software based on the branch-and-cut algorithm is readily available [25], which is advantageous for practical implementation purposes.

Thus, compared to previous closely related works [16]–[21], the main modeling and methodological novelties of the proposed approach are 1) the characterization of the long-term uncertainty in transmission and distribution demand growth, 2) the consideration of an extended set of candidate assets that includes renewable-based generators at both the transmission and distribution levels, 3) the use of a linearized ac model for the distribution network, and 4) the application of mixed-integer linear programming under a scenario-based stochastic programming framework. Table I summarizes the above-described differences between this work and the state of the art [16]–[21]. In this table, "T&D" stands for transmission and distribution, whereas symbols "✓" and "×" respectively indicate whether a particular aspect is considered or not.

Within the context of integrated transmission and distribution system planning, the main contributions of this paper are as follows:

1) For the first time in the literature, investment decisions on conventional generation, renewable-based generation, and network assets at both the transmission and distribution levels are co-optimized.
2) The long-term uncertainty associated with demand growth and the short-term uncertainty related to the variability of demand and renewable-based generation are jointly considered under a scenario-based stochastic programming framework.
3) A study of the benefits of the proposed model is presented for several cases. This study demonstrates the effective performance of the proposed approach and the impact of uncertainty and distributed generation on investment decisions, while providing insight into the economic gain over a practical sequential approach.

The use of the integrated approach presented here overcomes the weaknesses associated with the functional decoupling of transmission and distribution network planning currently implemented in industry practice, which may lead to economic losses, reduced reliability, and a suboptimal use of resources. As a result, the various stakeholders, regulators, and practitioners are provided with the globally optimal investment decisions, from a system-wide perspective, under the long-term uncertainty in demand growth and the short-term uncertainty associated with demand and renewable-based

generation. From a practical viewpoint, the proposed approach may be useful to system planners and regulators in two respects. First, alternative strategies for the coordination and interaction between transmission and distribution investments could be assessed using the resulting integrated expansion plan as a benchmark. In addition, the integrated expansion plan may provide relevant information to determine suitable investments that would require appropriate incentives for investors for their eventual installation. Note that the design of such incentive mechanisms is beyond the scope of this paper.

The rest of this paper is organized as follows. In Section II, uncertainty modeling is characterized. Section III presents the formulation for the proposed stochastic programming problem. Numerical results are analyzed and discussed in Section IV. Finally, some relevant conclusions are drawn in Section V.

II. Uncertainty Modeling

Within an expansion planning context, the characterization of both long- and short-term uncertainty sources is essential particularly in the current transition toward a decarbonized framework relying on highly variable renewable-based generation. Here, we model the long-term uncertainty associated with demand growth as well as the short-term uncertainty associated with demand and renewable-based generation.

For the long-term uncertainty, we propose the use of scenarios representing demand growth forecasts [26]. Each long-term scenario ω is associated with a demand growth factor μ_{ω}^{LG} and its corresponding probability of occurrence π_{ω}.

For the short-term uncertainty, we propose the use of historical data, namely hourly observations, to generate a set of scenarios capturing the correlation of uncertain demand and renewable-based power generation at each node of both system levels. First, these data are expressed as per-unit factors by dividing them by the corresponding maximum level (peak demand and maximum value of renewable-based power generation). Hence, each set of factors represents the per-unit demand and renewable-based power production profile at each node. Subsequently, with the purpose of better characterizing the different operating conditions, the set of per-unit historical observations is divided into N_B time blocks, e.g., according to the seasons of the year. Finally, the k-means++ algorithm [23] is applied to the set of observations of each time block, thereby obtaining a pre-specified number of scenarios.

The k-means++ clustering technique combines the conventional k-means method with a randomized initialization technique that improves speed and accuracy. In essence, k-means++ is an iterative algorithm aiming to reduce the initial data set composed of multiple observations by grouping them into a pre-specified number of clusters, representing the scenarios.

The step-by-step application of the k-means++ clustering technique to each time block b is described below using the following notation. Observations are indexed by o and $\mathcal{O}_b$ is the index set of observations for time block b $\{\phi_{nbo}^{L}, \phi_{nbo}^{W}\}_{\forall n \in (\mathcal{N}^T \cup \mathcal{N}^D)}$, where ϕ_{nbo}^{L} and ϕ_{nbo}^{W} respectively denote the demand factor and the renewable-based power production factor at node n, time block b, and observation o. In addition, K is the pre-specifed number of clusters, which are indexed by k, $\mathcal{O}_{bk}^{C}$ denotes the index set of observations grouped in cluster k for time block b, c_{bk} represents the centroid of cluster k for time block b, and d_{bo} is the shortest distance between observation o and the closest centroid for time block b. Based on [23], the k-means++ algorithm comprises the following steps:

Step 1) Set k equal to 1 and the initial centroid, $c_{b1} = \{\mu_{nb1}^{L}, \mu_{nb1}^{W}\}_{\forall n \in (\mathcal{N}^T \cup \mathcal{N}^D)}$, to be equal to the value of the oth observation $\{\phi_{nbo}^{L}, \phi_{nbo}^{W}\}_{\forall n \in (\mathcal{N}^T \cup \mathcal{N}^D)}$, with o randomly picked from $\mathcal{O}_b$ assuming that all observations are equiprobable.

Step 2) Set $k \leftarrow k + 1$ and the next centroid k, $c_{bk} = \{\mu_{nbk}^{L}, \mu_{nbk}^{W}\}_{\forall n \in (\mathcal{N}^T \cup \mathcal{N}^D)}$, to be equal to the value of the oth observation $\{\phi_{nbo}^{L}, \phi_{nbo}^{W}\}_{\forall n \in (\mathcal{N}^T \cup \mathcal{N}^D)}$, with o randomly picked from $\mathcal{O}_b$ considering that the probability for each observation o is equal to $\frac{d_{bo}^2}{\sum_{o' \in \mathcal{O}_b} d_{bo'}^2}$.

Step 3) Repeat Step 2 until K centroids are identified.

Step 4) Assign observations $\{\phi_{nbo}^{L}, \phi_{nbo}^{W}\}_{\forall n \in (\mathcal{N}^T \cup \mathcal{N}^D), \forall o \in \mathcal{O}_b}$ to the corresponding closest centroid c_{bk}, thereby giving rise to K clusters.

Step 5) For each cluster k, compute a new centroid as $c_{bk} = \{\mu_{nbk}^{L}, \mu_{nbk}^{W}\}_{\forall n \in (\mathcal{N}^T \cup \mathcal{N}^D)}$ using the average values of the factors for demand and renewable-based generation of the observations within the cluster, i.e., $\mu_{nbk}^{L} = \frac{1}{|\mathcal{O}_{bk}^{C}|} \sum_{o \in \mathcal{O}_{bk}^{C}} \phi_{nbo}^{L}$ and $\mu_{nbk}^{W} = \frac{1}{|\mathcal{O}_{bk}^{C}|} \sum_{o \in \mathcal{O}_{bk}^{C}} \phi_{nbo}^{W}$, $\forall n \in (\mathcal{N}^T \cup \mathcal{N}^D)$.

Step 6) Repeat Steps 4 and 5 until the centroids no longer change.

For each time block b, each cluster k yields a short-term uncertainty scenario s, which is represented by the value of the corresponding centroid $\{\mu_{nbs}^{L}, \mu_{nbs}^{W}\}_{\forall n \in (\mathcal{N}^T \cup \mathcal{N}^D)}$ and the number of hours associated with the observations grouped by the corresponding cluster, Δ_{bs}.

III. Stochastic Programming Model

The co-optimized expansion planning model under uncertainty is formulated as an instance of stochastic programming [22]. As is customary in power system planning [27], [28], a static approach focusing on a single target year is adopted. In addition, nodal uncertainty is characterized by a set of scenarios, which are generated as described in Section II.

Under the proposed integrated framework, the entity responsible for system-wide planning decisions has access to all data, which is consistent with industry practice [4], [5]. Note that the correspondence of both existing and candidate assets to each distribution network is modeled by the related index sets, which are known as done in the extensive body of literature on distribution network planning [3] and the recent references on expansion planning jointly considering transmission and distribution systems [16]–[21].

Moreover, network effects are characterized by two approximate models. For the transmission network, the widely used dc load flow [29] is adopted. For the distribution level, a

linearized ac load flow [30], [31] is used. For the sake of simplicity, losses are neglected at both levels. As compared with more accurate approximations such as that based on second-order cone programming (SOCP) [32], [33], the use of the proposed simpler power flow model for the distribution level allows leveraging efficient off-the-shelf software for mixed-integer linear programming [25], yet bringing out the main features of reactive power. Within the proposed scenario-based integrated approach involving several distribution systems, the consideration of an approximate SOCP-based power flow model would require the convexification of as many power flows as the number of scenarios times the number of distribution systems. Thus, even for moderately sized systems, the resulting mixed-integer quadratically-constrained program would be computationally challenging and would likely lead to intractability for state-of-the-art SOCP solution algorithms and current computing capabilities. Finally, the radial topology of the distribution network is explicitly imposed. According to [22], the stochastic programming model can be mathematically formulated as a scenario-based deterministic equivalent, as described next.

We recognize that the application of the model presented in this paper leads to results that may be optimistic. Therefore, a complete study would require the consideration of 1) more sophisticated operational models, and 2) alternative coordination schemes characterizing other types of interaction between the different agents involved while also preserving information confidentiality. These limitations notwithstanding, the use of our model is interesting for integrated transmission and distribution planning purposes and provides stakeholders with valuable information about the most economically efficient investment plan.

A. Objective Function and Cost-Related Terms

The goal of the proposed model is the minimization of the expected total cost, which is formulated as follows:

$$c^{T} = c^{I,T} + c^{O,T} + c^{I,D} + c^{O,D}. \tag{1}$$

The expected total cost in (1) comprises the annualized investment costs and the expected operating costs for both the transmission and distribution levels. Such cost terms are formulated as follows:

$$c^{I,T} = \sum_{p\in\mathcal{P}^T}\sum_{g\in\mathcal{G}_p^{T+}} IC_{gp}^{G,T} x_{gp}^{G,T} + \sum_{l\in\mathcal{L}^{T+}} IC_{l}^{L,T} x_{l}^{L,T} \tag{2}$$

$$c^{O,T} = \sum_{\omega\in\Omega}\pi_\omega \sum_{b\in\mathcal{B}}\sum_{s\in\mathcal{S}_b}\Delta_{bs}\left(\sum_{p\in\mathcal{P}^T}\sum_{g\in\left(\mathcal{G}_p^{T}\cup\mathcal{G}_p^{T+}\right)} OC_{gp}^{G,T} p_{gpbs\omega}^{G,T} + \sum_{d\in\mathcal{D}^T} OC_{d}^{U,T} p_{dbs\omega}^{U,T}\right) \tag{3}$$

$$c^{I,D} = \sum_{p\in\mathcal{P}^D}\sum_{g\in\mathcal{G}_p^{D+}} IC_{gp}^{G,D} x_{gp}^{G,D} + \sum_{l\in\mathcal{L}^{D+}} IC_{l}^{L,D} x_{l}^{L,D} \tag{4}$$

$$c^{O,D} = \sum_{\omega\in\Omega}\pi_\omega \sum_{b\in\mathcal{B}}\sum_{s\in\mathcal{S}_b}\Delta_{bs}\left(\sum_{p\in\mathcal{P}^D}\sum_{g\in\left(\mathcal{G}_p^{D}\cup\mathcal{G}_p^{D+}\right)} OC_{gp}^{G,D} p_{gpbs\omega}^{G,D} + \sum_{d\in\mathcal{D}^D} OC_{d}^{U,D} p_{dbs\omega}^{U,D}\right). \tag{5}$$

Expression (2) represents the annualized transmission investment cost, which comprises two terms related to the installation of new generators and transmission lines, respectively. In (3), the expected transmission operating cost is formulated as the sum of the expected costs of production and load shedding. Expressions (4) and (5) are respectively analogous to (2) and (3) for the distribution system.

B. Investment Constraints

The constraints associated with investment decisions are formulated as:

$$x_{l}^{L,T} \in \{0,1\};\ \forall l \in \mathcal{L}^{T+} \tag{6}$$

$$x_{l}^{L,D} \in \{0,1\};\ \forall l \in \mathcal{L}^{D+} \tag{7}$$

$$x_{gp}^{G,T} \le \overline{X}_{gp}^{G,T};\ \forall g \in \mathcal{G}_p^{T+}, \forall p \in \mathcal{P}^T \tag{8}$$

$$x_{gp}^{G,D} \le \overline{X}_{gp}^{G,D};\ \forall g \in \mathcal{G}_p^{D+}, \forall p \in \mathcal{P}^D \tag{9}$$

$$c^{I,T} + c^{I,D} \le \overline{IC}. \tag{10}$$

Constraints (6) and (7) set the binary nature of the variables modeling investments in transmission and distribution lines, respectively. Constraints (8) and (9) impose the upper bounds for generation investment at the transmission and distribution levels, respectively. Finally, an annualized budgetary limit for investments is modeled in (10).

C. Transmission System Operation

This section is devoted to the operation of transmission system components except the nodes where a distribution system is connected through the corresponding substation. These nodes, hereinafter referred to as interface nodes, are characterized in Section III-E. For the other transmission components, the operational model comprises the following set of constraints:

$$\sum_{p\in\mathcal{P}^T}\sum_{g\in\left(\mathcal{G}_{pn}^{T}\cup\mathcal{G}_{pn}^{T+}\right)} p_{gpbs\omega}^{G,T} - \sum_{\substack{l\in\left(\mathcal{L}^{T}\cup\mathcal{L}^{T+}\right)\\ |fr(l)=n}} p_{lbs\omega}^{L,T} + \sum_{\substack{l\in\left(\mathcal{L}^{T}\cup\mathcal{L}^{T+}\right)\\ |to(l)=n}} p_{lbs\omega}^{L,T} = \sum_{d\in\mathcal{D}_n^T}\left(\mu_\omega^{LG}\mu_{nbs}^{L} P_d^{D,T} - p_{dbs\omega}^{U,T}\right);$$
$$\forall n \in \left(\mathcal{N}^T\backslash\mathcal{N}^\infty\right), \forall b \in \mathcal{B}, \forall s \in \mathcal{S}_b, \forall \omega \in \Omega \tag{11}$$

$$p_{lbs\omega}^{L,T} = \frac{1}{X_l^T}\left[\delta_{fr(l)bs\omega} - \delta_{to(l)bs\omega}\right];$$
$$\forall l \in \mathcal{L}^{T}, \forall b \in \mathcal{B}, \forall s \in \mathcal{S}_b, \forall \omega \in \Omega \tag{12}$$

$$p_{lbs\omega}^{L,T} = \frac{x_l^{L,T}}{X_l^T}\left[\delta_{fr(l)bs\omega} - \delta_{to(l)bs\omega}\right];$$
$$\forall l \in \mathcal{L}^{T+}, \forall b \in \mathcal{B}, \forall s \in \mathcal{S}_b, \forall \omega \in \Omega \tag{13}$$

$$\delta_{nbs\omega} = 0;\ \forall n : \text{ref.}, \forall b \in \mathcal{B}, \forall s \in \mathcal{S}_b, \forall \omega \in \Omega \tag{14}$$

$$-\overline{P}_l^{L,T} \le p_{lbs\omega}^{L,T} \le \overline{P}_l^{L,T};\ \forall l \in \mathcal{L}^T, \forall b \in \mathcal{B} \quad \forall s \in \mathcal{S}_b, \forall \omega \in \Omega \tag{15}$$

$$-\overline{P}_l^{L,T} x_l^{L,T} \le p_{lbs\omega}^{L,T} \le \overline{P}_l^{L,T} x_l^{L,T};\quad \forall l \in \mathcal{L}^{T+}, \forall b \in \mathcal{B}, \forall s \in \mathcal{S}_b, \forall \omega \in \Omega \tag{16}$$

$$0 \le p_{gpbs\omega}^{G,T} \le \overline{P}_{gp}^{G,T};\quad \forall g \in \mathcal{G}_p^T, \forall p \in C^T, \forall b \in \mathcal{B}, \forall s \in \mathcal{S}_b, \forall \omega \in \Omega \tag{17}$$

$$0 \le p_{gpbs\omega}^{G,T} \le x_{gp}^{G,T};\quad \forall g \in \mathcal{G}_p^{T+}, \forall p \in C^T, \forall b \in \mathcal{B}, \forall s \in \mathcal{S}_b, \forall \omega \in \Omega \tag{18}$$

$$0 \le p_{gpbs\omega}^{G,T} \le \mu_{nbs}^W \overline{P}_{gp}^{G,T};\quad \forall n \in \mathcal{N}^T, \forall g \in \mathcal{G}_{pn}^T, \forall p \in W^T, \forall b \in \mathcal{B}, \forall s \in \mathcal{S}_b, \forall \omega \in \Omega \tag{19}$$

$$0 \le p_{gpbs\omega}^{G,T} \le \mu_{nbs}^W x_{gp}^{G,T};\quad \forall n \in \mathcal{N}^T, \forall g \in \mathcal{G}_{pn}^{T+}, \forall p \in W^T, \forall b \in \mathcal{B}, \forall s \in \mathcal{S}_b, \forall \omega \in \Omega \tag{20}$$

$$0 \le p_{dbs\omega}^{U,T} \le \mu_{\omega}^{LG} \mu_{nbs}^L P_d^{D,T};\quad \forall n \in \mathcal{N}^T, \forall d \in \mathcal{D}_n^T, \forall b \in \mathcal{B}, \forall s \in \mathcal{S}_b, \forall \omega \in \Omega. \tag{21}$$

The effect of the transmission network is characterized in (11)–(13) by a linearized dc network model commonly used in transmission network planning. Expressions (11) model the power balances for all transmission nodes excluding interface nodes. Power flows across existing and candidate transmission lines are formulated in (12) and (13), respectively. Note that expressions (13) include nonlinearities related to bilinear terms involving the products of continuous and binary decision variables that can be linearized as described in Section III-F. The voltage angles at the reference node are set in (14). Constraints (15)–(20) impose the upper and lower bounds on flows and injections for the existing and candidate assets in the transmission system, namely lines as well as conventional and renewable-based generators. Finally, nodal load shedding is bounded in (21).

D. Distribution System Operation

Distribution system operation is formulated as follows:

$$\sum_{p \in \mathcal{P}^D} \sum_{g \in \left(\mathcal{G}_{pn}^D \cup \mathcal{G}_{pn}^{D+}\right)} p_{gpbs\omega}^{G,D} - \sum_{\substack{l \in (\mathcal{L}^D \cup \mathcal{L}^{D+}) \\ |fr(l)=n}} p_{lbs\omega}^{L,D} + \sum_{\substack{l \in (\mathcal{L}^D \cup \mathcal{L}^{D+}) \\ |to(l)=n}} p_{lbs\omega}^{L,D} = \sum_{d \in \mathcal{D}_n^D} \left(\mu_{\omega}^{LG} \mu_{nbs}^L P_d^{D,D} - p_{dbs\omega}^{U,D}\right);\quad \forall n \in \mathcal{N}^D, \forall b \in \mathcal{B}, \forall s \in \mathcal{S}_b, \forall \omega \in \Omega \tag{22}$$

$$\sum_{p \in \mathcal{P}^D} \sum_{g \in \left(\mathcal{G}_{pn}^D \cup \mathcal{G}_{pn}^{D+}\right)} q_{gpbs\omega}^{G,D} - \sum_{\substack{l \in (\mathcal{L}^D \cup \mathcal{L}^{D+}) \\ |fr(l)=n}} q_{lbs\omega}^{L,D} + \sum_{\substack{l \in (\mathcal{L}^D \cup \mathcal{L}^{D+}) \\ |to(l)=n}} q_{lbs\omega}^{L,D} = \tan^{-1}(\rho_{nb}) \sum_{d \in \mathcal{D}_n^D} \left(\mu_{\omega}^{LG} \mu_{nbs}^L P_d^{D,D} - p_{dbs\omega}^{U,D}\right);\quad \forall n \in \mathcal{N}^D, \forall b \in \mathcal{B}, \forall s \in \mathcal{S}_b, \forall \omega \in \Omega \tag{23}$$

$$v_{to(l)bs\omega} - v_{fr(l)bs\omega} + 2\left(R_l^D p_{lbs\omega}^{L,D} + X_l^D q_{lbs\omega}^{L,D}\right) = 0;\quad \forall l \in \mathcal{L}^D, \forall b \in \mathcal{B}, \forall s \in \mathcal{S}_b, \forall \omega \in \Omega \tag{24}$$

$$x_l^{L,D}\left[v_{to(l)bs\omega} - v_{fr(l)bs\omega} + 2\left(R_l^D p_{lbs\omega}^{L,D} + X_l^D q_{lbs\omega}^{L,D}\right)\right] = 0;\quad \forall l \in \mathcal{L}^{D+}, \forall b \in \mathcal{B}, \forall s \in \mathcal{S}_b, \forall \omega \in \Omega \tag{25}$$

$$\left(\underline{V}^D\right)^2 \le v_{nbs\omega} \le \left(\overline{V}^D\right)^2;\quad \forall n \in \mathcal{N}^D, \forall b \in \mathcal{B}, \forall s \in \mathcal{S}_b, \forall \omega \in \Omega \tag{26}$$

$$-\overline{S}_l^{L,D} \le p_{lbs\omega}^{L,D} \le \overline{S}_l^{L,D};\ \forall l \in \mathcal{L}^D, \forall b \in \mathcal{B}, \forall s \in \mathcal{S}_b, \forall \omega \in \Omega \tag{27}$$

$$-\overline{S}_l^{L,D} \le q_{lbs\omega}^{L,D} \le \overline{S}_l^{L,D};\ \forall l \in \mathcal{L}^D, \forall b \in \mathcal{B}, \forall s \in \mathcal{S}_b, \forall \omega \in \Omega \tag{28}$$

$$-\overline{S}_l^{L,D} x_l^{L,D} \le p_{lbs\omega}^{L,D} \le \overline{S}_l^{L,D} x_l^{L,D};\quad \forall l \in \mathcal{L}^{D+}, \forall b \in \mathcal{B}, \forall s \in \mathcal{S}_b, \forall \omega \in \Omega \tag{29}$$

$$-\overline{S}_l^{L,D} x_l^{L,D} \le q_{lbs\omega}^{L,D} \le \overline{S}_l^{L,D} x_l^{L,D};\quad \forall l \in \mathcal{L}^{D+}, \forall b \in \mathcal{B}, \forall s \in \mathcal{S}_b, \forall \omega \in \Omega \tag{30}$$

$$0 \le p_{gpbs\omega}^{G,D} \le \overline{S}_{gp}^{G,D};\quad \forall g \in \mathcal{G}_p^D, \forall p \in C^D, \forall b \in \mathcal{B}, \forall s \in \mathcal{S}_b, \forall \omega \in \Omega \tag{31}$$

$$-\overline{S}_{gp}^{G,D} \le q_{gpbs\omega}^{G,D} \le \overline{S}_{gp}^{G,D};\quad \forall g \in \mathcal{G}_p^D, \forall p \in C^D, \forall b \in \mathcal{B}, \forall s \in \mathcal{S}_b, \forall \omega \in \Omega \tag{32}$$

$$0 \le p_{gpbs\omega}^{G,D} \le x_{gp}^{G,D};\quad \forall g \in \mathcal{G}_p^{D+}, \forall p \in C^D, \forall b \in \mathcal{B}, \forall s \in \mathcal{S}_b, \forall \omega \in \Omega \tag{33}$$

$$-x_{gp}^{G,D} \le q_{gpbs\omega}^{G,D} \le x_{gp}^{G,D};\quad \forall g \in \mathcal{G}_p^{D+}, \forall p \in C^D, \forall b \in \mathcal{B}, \forall s \in \mathcal{S}_b, \forall \omega \in \Omega \tag{34}$$

$$0 \le p_{gpbs\omega}^{G,D} \le \mu_{nbs}^W \overline{S}_{gp}^{G,D};\ \forall n \in \mathcal{N}^D, \forall g \in \mathcal{G}_{pn}^D, \forall p \in W^D, \forall b \in \mathcal{B}, \forall s \in \mathcal{S}_b, \forall \omega \in \Omega \tag{35}$$

$$-\mu_{nbs}^W \overline{S}_{gp}^{G,D} \le q_{gpbs\omega}^{G,D} \le \mu_{nbs}^W \overline{S}_{gp}^{G,D};\ \forall n \in \mathcal{N}^D, \forall g \in \mathcal{G}_{pn}^D, \forall p \in W^D, \forall b \in \mathcal{B}, \forall s \in \mathcal{S}_b, \forall \omega \in \Omega \tag{36}$$

$$0 \le p_{gpbs\omega}^{G,D} \le \mu_{nbs}^W x_{gp}^{G,D};\ \forall n \in \mathcal{N}^D, \forall g \in \mathcal{G}_{pn}^{D+}, \forall p \in W^D, \forall b \in \mathcal{B}, \forall s \in \mathcal{S}_b, \forall \omega \in \Omega \tag{37}$$

$$-\mu_{nbs}^W x_{gp}^{G,D} \le q_{gpbs\omega}^{G,D} \le \mu_{nbs}^W x_{gp}^{G,D};\ \forall n \in \mathcal{N}^D, \forall g \in \mathcal{G}_{pn}^{D+}, \forall p \in W^D, \forall b \in \mathcal{B}, \forall s \in \mathcal{S}_b, \forall \omega \in \Omega \tag{38}$$

$$0 \le p_{dbs\omega}^{U,D} \le \mu_{\omega}^{LG} \mu_{nbs}^L P_d^{D,D};\quad \forall n \in \mathcal{N}^D, \forall d \in \mathcal{D}_n^D, \forall b \in \mathcal{B}, \forall s \in \mathcal{S}_b, \forall \omega \in \Omega \tag{39}$$

$$\sum_{n \in \mathcal{N}_a^{D+}} \sum_{\substack{l \in \mathcal{L}^{D+} \\ |(fr(l)=n \vee to(l)=n)}} x_l^{L,D} = \text{card}(\mathcal{N}_a^{D+});\ \forall a \in \mathcal{A}. \tag{40}$$

Constraints (22)–(25) represent a linearized ac network model that is suitable for radial distribution networks [30]. Active and reactive power balances at distribution nodes are modeled in (22) and (23), respectively. Constraints (24) and (25) relate nodal voltages to the active and reactive power flows across existing and candidate distribution lines, respectively. Similar to (13), constraints (25) feature nonlinearities, for which a linear equivalent is provided in Section III-F. In

addition, constraints (26) limit voltage magnitudes for distribution nodes. Constraints (27)–(39) impose the upper and lower bounds on active and reactive power flows and injections for the existing and candidate assets in the distribution system, namely lines as well as conventional and renewable-based generators. Based on [31] and [33], expressions (27)–(38) represent linear approximations of the apparent power limits coupling active and reactive power flows and injections. Note that, as done in [31] and [33], both active and reactive power flows across distribution lines are limited by their maximum levels of apparent power flow in (27)–(30). Analogously, as an extension of the model used for distribution lines, the active and reactive power outputs of distributed generators are also bounded by their corresponding maximum levels of apparent power production, as modeled in (31)–(38). Expressions (39) bound load shedding. Finally, expressions (40) preserve the radial topology for every expanded distribution network. This result, which is a consequence of the cost minimization driving the optimization process, relies on the practical assumption that, at new disconnected load nodes, local generation is insufficient to supply the corresponding nodal demand.

E. Interface Node Operation

The operation of interface nodes is modeled by the following constraints:

$$\begin{aligned}&\sum_{p\in\mathcal{P}^T}\sum_{g\in\left(\mathcal{G}^T_{pn}\cup\mathcal{G}^{T+}_{pn}\right)} p^{G,T}_{gpbs\omega} - \sum_{\substack{l\in(\mathcal{L}^T\cup\mathcal{L}^{T+})\\ |fr(l)=n}} p^{L,T}_{lbs\omega} \\ &\quad + \sum_{\substack{l\in(\mathcal{L}^T\cup\mathcal{L}^{T+})\\ |to(l)=n}} p^{L,T}_{lbs\omega} - \sum_{\substack{l\in(\mathcal{L}^D\cup\mathcal{L}^{D+})\\ |fr(l)=n}} p^{L,D}_{lbs\omega} \\ &\quad + \sum_{\substack{l\in(\mathcal{L}^D\cup\mathcal{L}^{D+})\\ |to(l)=n}} p^{L,D}_{lbs\omega} \\ &= \sum_{d\in\mathcal{D}^T_n}\left(\mu^{LG}_{\omega}\mu^{L}_{nbs}P^{D,T}_{d} - p^{U,T}_{dbs\omega}\right); \\ &\quad \forall n\in\mathcal{N}^{\infty},\forall b\in\mathcal{B},\forall s\in\mathcal{S}_b,\forall\omega\in\Omega \qquad (41)\end{aligned}$$

$$v_{nbs\omega}=1;\ \forall n\in\mathcal{N}^{\infty},\forall b\in\mathcal{B},\forall s\in\mathcal{S}_b,\forall\omega\in\Omega. \qquad (42)$$

Constraints (41) correspond to the power balance equations at those nodes connecting the transmission and distribution levels. As can be observed, power flows across both transmission and distribution lines are accounted for in (41), thereby explicitly modeling the connection between both levels. Finally, according to the assumptions made for the linearized dc network model used for the transmission system, constraints (42) set the voltage magnitude at interface nodes equal to 1.

F. Mixed-Integer Linear Formulation

The proposed stochastic model is a mixed-integer nonlinear program that can be recast as an instance of mixed-integer linear programming by replacing nonlinear expressions (13) and (25) with linear terms. Using the disjunctive-constraint-based transformation described in [29], nonlinear expressions (13) and (25) have the following linear equivalents:

$$\begin{aligned}&-M^T\left(1-x^{L,T}_l\right)\le p^{L,T}_{lbs\omega}-\frac{1}{X^T_l}\left[\delta_{fr(l)bs\omega}-\delta_{to(l)bs\omega}\right] \\ &\quad\le M^T\left(1-x^{L,T}_l\right);\ \forall l\in\mathcal{L}^{T+},\forall b\in\mathcal{B},\forall s\in\mathcal{S}_b,\forall\omega\in\Omega \qquad (43)\end{aligned}$$

$$\begin{aligned}&-M^D\left(1-x^{L,D}_l\right) \\ &\quad\le v_{to(l)bs\omega}-v_{fr(l)bs\omega}+2\left(R^D_l p^{L,D}_{lbs\omega}+X^D_l q^{L,D}_{lbs\omega}\right) \\ &\quad\le M^D\left(1-x^{L,D}_l\right);\ \forall l\in\mathcal{L}^{D+},\forall b\in\mathcal{B},\forall s\in\mathcal{S}_b,\forall\omega\in\Omega. \qquad (44)\end{aligned}$$

If $x^{L,T}_l$ is equal to 1, the corresponding constraint (43) becomes $0\le p^{L,T}_{lbs\omega}-\frac{1}{X^T_l}[\delta_{fr(l)bs\omega}-\delta_{to(l)bs\omega}]\le 0$, which is identical to the condition $p^{L,T}_{lbs\omega}=\frac{1}{X^T_l}[\delta_{fr(l)bs\omega}-\delta_{to(l)bs\omega}]$ resulting from (13). Conversely, if $x^{L,T}_l$ is equal to 0, the corresponding constraint (43) yields $-M^T\le p^{L,T}_{lbs\omega}-\frac{1}{X^T_l}[\delta_{fr(l)bs\omega}-\delta_{to(l)bs\omega}]\le M^T$, i.e., $|\delta_{fr(l)bs\omega}-\delta_{to(l)bs\omega}|\le M^T$, since $p^{L,T}_{lbs\omega}$ is equal to 0 as per (16). Thus, for a sufficiently large positive value for parameter M^T, no relation between nodal phase angles $\delta_{fr(l)bs\omega}$ and $\delta_{to(l)bs\omega}$ is imposed, as modeled in (13) for $x^{L,T}_l$ equal to 0. Analogously, if $x^{L,D}_l$ is equal to 1, the corresponding constraint (44) becomes $0\le v_{to(l)bs\omega}-v_{fr(l)bs\omega}+2(R^D_l p^{L,D}_{lbs\omega}+X^D_l q^{L,D}_{lbs\omega})\le 0$, which is identical to the condition $v_{to(l)bs\omega}-v_{fr(l)bs\omega}+2(R^D_l p^{L,D}_{lbs\omega}+X^D_l q^{L,D}_{lbs\omega})=0$ resulting from (25). Conversely, if $x^{L,D}_l$ is equal to 0, the corresponding constraint (44) yields $-M^D\le v_{to(l)bs\omega}-v_{fr(l)bs\omega}\le M^D$, i.e., $|v_{to(l)bs\omega}-v_{fr(l)bs\omega}|\le M^D$, since $p^{L,D}_{lbs\omega}$ and $q^{L,D}_{lbs\omega}$ are equal to 0 as per (29) and (30), respectively. Thus, for a sufficiently large positive value for parameter M^D, no relation between nodal voltage magnitudes $v_{fr(l)bs\omega}$ and $v_{to(l)bs\omega}$ is imposed, as modeled in (25) for $x^{L,D}_l$ equal to 0.

For the sake of completeness, the resulting mixed-integer linear program is formulated as:

$$\underset{\substack{c^T,c^{I,D},c^{I,T},c^{O,D},c^{O,T},p^{G,D}_{gpbs\omega},\\ p^{G,T}_{gpbs\omega},p^{L,D}_{lbs\omega},p^{L,T}_{lbs\omega},p^{U,D}_{dbs\omega},p^{U,T}_{dbs\omega},q^{G,D}_{gpbs\omega},\\ q^{L,D}_{lbs\omega},v_{nbs\omega},\delta_{nbs\omega},x^{G,D}_{gp},x^{G,T}_{gp},x^{L,D}_{l},x^{L,T}_{l}}}{\text{Minimize}} \quad c^T \qquad (45)$$

subject to:

$$\text{Constraints (1)–(12), (14)–(24), and (26)–(44).} \qquad (46)$$

The proposed instance of mixed-integer linear programming is suitable for off-the-shelf software based on the state-of-the-art branch-and-cut algorithm [25].

IV. Results

This section presents and discusses results from two case studies. For proof-of-concept purposes, a 36-node test system is first analyzed. The scalability of the proposed approach is subsequently validated with a larger case study comprising 334 nodes.

The long-term uncertainty associated with demand growth and the short-term uncertainty related to the variability of demand and renewable-based generation are jointly considered in both case studies. Based on forecasts, three equiprobable realizations for demand growth are accounted for. The characterization of both short-term uncertainty sources relies on historical data. Each transmission node is subject to different demand and wind power profiles. For the sake of simplicity, it is assumed that each distribution node is subject to the same demand and wind power profiles as the interface transmission node where the corresponding distribution system is connected. Moreover, four seasonal time blocks are considered with durations equal to 2160 h/year, 2208 h/year, 2232 h/year, and 2160 h/year, respectively. For each time block, 35 different conditions of demand and wind power production are accounted for according to the procedure described in Section II. As a result, 420 scenarios (3 long-term uncertainty scenarios, 4 time blocks, and 35 short-term uncertainty scenarios per time block) are analyzed for the target year, which is consistent with industry practice in Spain [5]. Detailed information on the characterization of uncertain demand growth, nodal demands, and wind power generation is provided in [34].

For both case studies, existing generation assets only comprise conventional generating units whereas the fleet of candidate generators only includes wind-based generating units. According to (42), voltages at interface nodes, where substations are located, are set to 1.00 p.u., whereas upper and lower bounds for voltages at distribution nodes are equal to 1.05 p.u. and 0.95 p.u., respectively. The load-shedding cost coefficients, $OC_d^{U,T}$ and $OC_d^{U,D}$, are based on those provided in [35]. Note that the solutions reported hereinafter remain unaltered for larger values of these coefficients. For the sake of reproducibility, system data and results for both case studies are also available in [34].

In order to assess the impact of DG on the expansion planning of the overall system, both case studies are first solved disregarding existing and candidate DG units. Subsequently, existing DG units are considered and investment in DG is allowed. For computational purposes, the simulations for the mixed-integer linear models with DG have been initialized with the optimal solution for the corresponding model with no DG.

Additionally, for both case studies, results from the proposed integrated approach have been assessed with those provided by a sequential implementation based on industry practice in Spain [4], [5]. First, the expansion planning problem for each distribution system is solved for a given investment budget. The required values for the energy supplied by substations are based on those used in [36]. Subsequently, the transmission expansion planning problem is solved for a pre-specified transmission investment budget. For the sake of a fair assessment, the resulting investment plans have been compared with those from the proposed integrated approach for an overall investment budget equal to the sum of the distribution and transmission investment budgets considered in the separate models.

Finally, the suitability of the linearized ac distribution network model has been examined by implementing a modified version of the proposed planning model wherein the effect of the distribution network is characterized by the formulation presented in [33], which is based on second-order cone programming. This modified version is also used to compute more accurate values of the total expected costs for the solutions provided by the proposed approach. To that end, the resulting second-order cone program is solved with expansion decisions fixed to those featured by such solutions.

Simulations have been run on a Dell PowerEdge R920X64 with four Intel Xeon E7-4820 processors at 2.00 GHz and 768 GB of RAM using GAMS 29.1 [37]. The instances of mixed-integer linear programming were solved to optimality by the branch-and-cut algorithm implemented in CPLEX 12.9 [25], i.e., the optimality gap was set to 0%. Note that using larger optimality gaps may yield significant computational savings. The alternative instances of second-order cone programming were solved using Gurobi 9.0 [38], which, according to [13], computationally outperforms CPLEX for this kind of problems. The execution of Gurobi was stopped when either the optimal solution was found or a time limit of one week was reached.

A. Illustrative Example

Fig. 1(a) depicts the one-line diagram of the test system, which is composed of a transmission system based on that described in [39] and two distribution systems. The transmission system comprises 6 nodes, represented by long bars, and 14 lines, indicated by thick lines. Both distribution systems are topologically identical and each comprises 15 nodes, depicted as short bars, and 23 lines, denoted by thin lines. Such distribution systems are connected to interface nodes 4 and 5, respectively. Note that transmission node 6 and distribution nodes 48, 58, 415, and 515 are not initially connected to the system.

Lines and generators in transmission and distribution systems are categorized as existing and candidate. Existing lines are represented by solid lines in Fig. 1(a) whereas candidate lines are drawn as dashed red lines. As shown in Fig. 1(a), existing generators are located at nodes 1, 3, 6, 44, 54, 411, and 511. In addition, transmission node 1 is a candidate location for the installation of wind-based generation with an upper limit equal to 250 MVA, which is also depicted in red, whereas all distribution nodes are candidate locations for the installation of wind power generators with an upper limit equal to 5 MVA per node. For quick reference, additional information on line and generation capacities is provided in Fig. 1(a). The annualized investment budget is $25 million.

The attainment of optimality required 191.5 s for the case without DG and 402.9 s for the case with DG. It should be noted that, for the latter, initializing CPLEX with the optimal solution for the case with no DG gave rise to a considerable 34.5% computational gain. Figs. 1(b) and 1(c) respectively show the investment decisions and topologies associated with the optimal solution for each case. Newly installed lines are depicted in orange whereas newly installed wind power generators are represented by blue icons. As can be observed, investment decisions in both systems significantly differ at both the transmission and distribution levels. For the case with DG, demand growth is partially compensated for by the installation of wind power generators at the distribution level. For

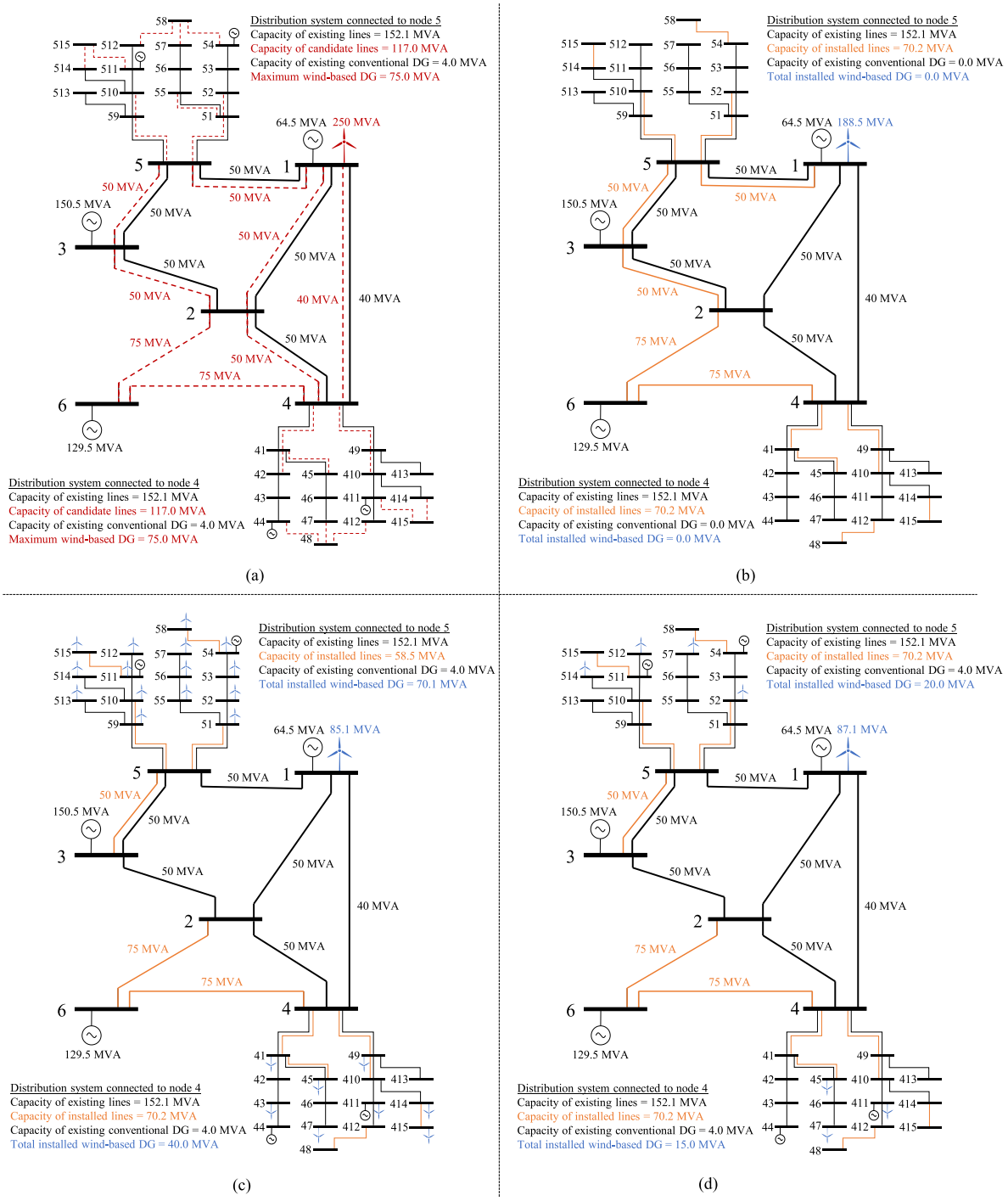

Fig. 1. 36-node system: (a) One-line diagram, (b) Optimal integrated investment plan without DG, (c) Optimal integrated investment plan with DG, (d) Optimal investment plan for the sequential approach with DG.

every installed wind power generator, the investment upper bound (5 MVA) is binding except for the new units at nodes 54, 55, and 511, for which 3.0 MVA, 2.9 MVA, and 4.2 MVA are installed, respectively. Note also that the consideration of DG prevents the installation of a second circuit in 1) the transmission corridors respectively connecting nodes 1 and 5 and nodes 2 and 3, and 2) the distribution corridor connecting nodes 51 and 52. Moreover, a further difference between both solutions arises in the distribution line connecting node 515 to the system. In addition, the total installed wind power generation grows from 188.5 MVA, for the case with no DG, up to 195.2 MVA, when DG is allowed. In other words, the consideration of DG increases the penetration of renewable-based generation by 3.55% over the case wherein DG is disregarded.

Table II lists the values of the different expected costs associated with the optimal solutions for both cases. As can be noted, the incorporation of DG yields a higher total generation investment cost. Moreover, for the case with no DG, the

TABLE II
36-NODE SYSTEM–EXPECTED COSTS (10^6 $)

Approach	Cost	Transmission level	Distribution level	Total
Integrated without DG	Generation investment	22.620	0.000	22.620
	Network investment	2.317	0.063	2.380
	Production	71.576	0.000	71.576
	Load shedding	0.000	6.682	6.682
	Total	96.513	6.745	103.258
Integrated with DG	Generation investment	10.214	13.182	23.396
	Network investment	1.545	0.059	1.604
	Production	65.691	3.794	69.485
	Load shedding	0.362	0.687	1.049
	Total	77.812	17.722	95.534
Sequential with DG	Generation investment	10.452	4.085	14.537
	Network investment	1.545	0.061	1.606
	Production	77.890	4.199	82.089
	Load shedding	0.000	2.060	2.060
	Total	89.887	10.405	100.292

generation expansion cost is solely incurred at the transmission level whereas, for the case with DG, part of this cost is shifted to the distribution level. The network investment costs at both system levels are lower when DG is considered and, therefore, the total network investment cost is reduced. Finally, both total production and load shedding costs are also lower for the case with DG. As a consequence, a 7.48% reduction in the total cost is attained by the solution with DG, which constitutes a total cost saving of $7.724 million.

Results from the application of the sequential approach to the case with DG are presented next. Investment budgets for the distribution systems connected to interface nodes 4 and 5 are $5 million and $8 million, respectively, whereas the investment budget for the transmission system is $12 million. Fig. 1(d) and Table II summarize the results for the sequential planning. As can be observed in Fig.1(d), the investment plan significantly differs as less distributed generation is installed as compared to that shown in Fig. 1(c) for the proposed integrated approach. Moreover, sequentially planning the systems requires the installation of a second circuit in the distribution corridor connecting nodes 51 and 52. The comparison of the results reported in Table II for the case with DG reveals that the proposed integrated approach attains a substantial 4.74% reduction in the expected total cost over that obtained by the sequential approach. This cost decrease mainly comes from the 15.35% reduction in the total production cost that outweighs the 60.94% increase in the total generation investment cost.

Confidence about the effective performance of the proposed approach can be gained by solving the case with DG while adopting a second-order cone programming model for the distribution network. By fixing the investment plan identified by the proposed approach in the second-order cone programming model, an expected total cost equal to $99.308 million was obtained. By contrast, for the more accurate planning model, the optimal expected total cost amounts to $98.244 million, as identified by Gurobi after 15295.6 s. It is worth mentioning that the proposed approach incurred a moderate 1.08% cost increase while significantly reducing the computational effort by 97.37%. Thus, this result corroborates that the use of the proposed linearized ac distribution network model is acceptable in terms of solution quality and computational burden.

TABLE III
36-NODE SYSTEM WITH DG–RESULTS OF THE OUT-OF-SAMPLE ASSESSMENT

	Proposed approach	Deterministic approach
Average sampled total cost (10^6 $)	92.359	599.890
CVaR of the sampled total costs (10^6 $)	125.772	2393.072

Moreover, the convenience of using a stochastic rather than a simpler deterministic solution approach is analyzed for the case with DG. To that end, a widely used metric, namely the value of the stochastic solution (VSS) [22], is calculated. For a minimization problem, the VSS is defined as the difference between two terms. The first term, denoted by c^{DP}, represents the value of the objective function obtained from the stochastic model by fixing decision variables not dependent on scenarios to the values resulting from solving the associated deterministic problem. Note that the solution for the deterministic model can be obtained by solving the stochastic model considering a single scenario for the uncertain parameters. The second term, denoted by c^{ST}, represents the value of the objective function resulting from the stochastic model. Thus, the VSS quantifies the potential gain associated with the stochastic solution. For the problem under consideration, c^{DP} is equal to the value of c^T obtained from solving the stochastic model (45)–(46) by fixing decision variables $x_{gp}^{G,D}$, $x_{gp}^{G,T}$, $x_l^{L,D}$, and $x_l^{L,T}$ to the values resulting from solving the deterministic model. For this particular case study, c^{DP} amounts to $900.238 million, whereas c^{ST} corresponds to the value of c^T provided by the stochastic model (45)–(46), which, as can be seen in Table II, is equal to $95.534 million. Thus, the VSS amounts to $804.704 million, which represents a potential 89.39% improvement upon the deterministic solution.

In order to further analyze the performance of the deterministic solution and the expansion decisions provided by the proposed stochastic approach, an out-of-sample assessment based on Monte Carlo simulation has been conducted for the case with DG. To that end, for the investment plans identified by both models, the optimal system operation has been determined for 10000 random samples of the uncertain parameters. For the generation of samples, the demand growth factor was characterized by a discrete function with values and probabilities equal to those used in the proposed approach. Nodal demand factors and nodal renewable-based power production factors were each characterized by a distribution function that was generated based on historical data using the commercial software @RISK [40]. Table III presents the out-of-sample results, namely the average sampled total cost and the conditional value-at-risk (CVaR) of the sampled total costs under a 95% confidence level, i.e., the average total cost over the 5% worst samples. As can be seen, the stochastic solution substantially outperformed the deterministic plan in terms of both metrics, thereby corroborating the superiority of the proposed approach.

TABLE IV
36-NODE SYSTEM WITH DG–IMPACT OF THE NUMBER OF SCENARIOS

Number of scenarios	Total cost (10^6 \$)	ϵ_C (%)	CPU time (s)	ϵ_T (%)
24	91.783	-3.93	1.5	-99.64
48	92.062	-3.63	6.2	-98.53
96	93.018	-2.63	23.9	-94.32
192	94.339	-1.25	64.9	-84.58
420	95.534	0.00	420.9	0.00
840	97.014	1.55	899.3	113.66
1260	97.850	2.42	5634.9	1238.77
1680	99.095	3.73	7404.9	1659.30
2100	99.623	4.28	13232.4	3043.83

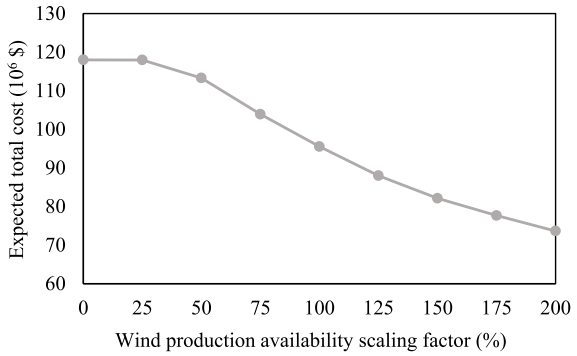

Fig. 2. 36-node system with DG: Expected value of the total cost versus level of wind power production availability.

Additionally, the effectiveness of using 420 scenarios has also been assessed for the case with DG. Table IV summarizes the results obtained by the proposed approach for several instances considering between 24 and 2100 scenarios. In columns 3 and 5, ϵ_C and ϵ_T respectively denote the percent cost and time differences in relation to the base instance, which corresponds to 420 scenarios. As can be observed, for relatively low numbers of scenarios, both the total costs and the simulation times are lower due to the imprecise characterization of extreme scenarios (high demand and low wind power production) and the reduced number of associated variables and constraints, respectively. For relatively larger numbers of scenarios, it can be seen that the total costs are slightly higher due to a better representation of the extreme scenarios at the expense of a significant increase in simulation times. Therefore, it can be concluded that, unlike [17], [19], and [21] where fewer than 40 scenarios were considered, the selected number of scenarios is suitable for the problem under consideration and gives rise to an acceptable trade-off between accuracy and computational tractability.

Finally, in order to analyze the effect of wind power production availability, the average factors for renewable-based power production, μ^W_{nbs}, have been scaled between 0% and 200% of their original values. Fig. 2 shows the optimal values of the expected total cost determined by the proposed approach for the case with DG. Note that the expected total cost decreases as the level of wind power production availability increases, thereby backing the economic benefit of renewable-based generation.

TABLE V
334-NODE SYSTEM–EXPECTED COSTS (10^6 \$)

Approach	Cost	Transmission level	Distribution level	Total
Integrated without DG	Generation investment	341.082	0.000	341.082
	Network investment	8.801	0.118	8.919
	Production	633.595	0.000	633.595
	Load shedding	0.000	39.419	39.419
	Total	983.478	39.537	1023.015
Integrated with DG	Generation investment	256.958	45.196	302.154
	Network investment	6.673	0.100	6.773
	Production	660.319	1.377	661.696
	Load shedding	0.317	0.000	0.317
	Total	924.267	46.673	970.940
Sequential with DG	Generation investment	256.848	11.823	268.671
	Network investment	8.158	0.105	8.263
	Production	696.166	1.259	697.425
	Load shedding	0.000	0.000	0.000
	Total	961.172	13.187	974.359

B. 334-Node Case Study

The second benchmark consists of a transmission system based on the IEEE 118-bus system [41] and 6 topologically identical distribution systems each based on that presented in [42]. The transmission system comprises 118 nodes and 147 lines. The distribution systems, each including 36 nodes and 46 lines, are connected to interface nodes 10, 21, 54, 62, 80, and 117.

For an investment budget equal to \$350 million, CPLEX required 10.65 h for the case without DG and 24.50 h for the case with DG. For this latter instance, the aforementioned initialization procedure of CPLEX yielded a lower albeit still significant 8.4% time reduction. Table V presents the economic results associated with both solutions. As can be observed, unlike in the illustrative example, the total production cost increases when DG is allowed. However, this cost increase is offset by the significant reductions in the total generation investment and load shedding costs. Note also that part of the generation investment and production costs are shifted from the transmission level to the distribution level while reducing the network investment costs at both levels. Overall, when DG is considered, the expected total cost is substantially decreased by 5.09%.

The case with DG has also been solved by the sequential approach based on industry practice. Investment budgets for the distribution systems connected to interface nodes 10, 21, 54, 62, 80, and 117 are \$0.012 million, \$0.018 million, \$20 million, \$20 million, \$24.97 million, and \$20 million, respectively, whereas the investment budget for the transmission system is \$265 million. Economic results for the sequential approach are also presented in Table V. The comparison of the results reported in Table V for the case with DG shows that the proposed integrated approach attains a 0.35% reduction in the expected total cost over that identified by the sequential approach. This cost decrease mainly comes from the 5.12% reduction in the total production cost along with the 18.03% reduction in the total network investment cost that offset the 12.46% increase in the total generation investment cost.

Finally, results from the application of second-order cone programming to the case with DG are presented. For comparison purposes, for the investment plan obtained by the proposed approach, the associated expected total cost using the second-order cone programming model was equal to $972.053 million. Unfortunately, for the resulting mixed-integer second-order cone program, Gurobi was unable to reduce the optimality gap under 29.94% after a with week (168 h). More importantly, the corresponding best feasible solution featured an expected total cost equal to $1384.841 million, thereby being 42.47% more expensive. These results substantiate the suitability of the proposed linearized ac distribution network model for large instances of the integrated planning problem under consideration.

V. Conclusion

This paper has investigated the integrated expansion planning of transmission and distribution systems considering investments in both network and generation assets. Both the long-term uncertainty in demand growth and the short-term uncertainty in demand and renewable-based power generation have been characterized through a stochastic programming framework based on a set of scenarios. The resulting integrated expansion planning model is a stochastic program whose associated scenario-based deterministic equivalent is cast as an instance of mixed-integer linear programming. Hence, finite convergence to optimality is guaranteed.

The proposed integrated tool allows identifying the expansion plan with the lowest possible system-wide expected cost while considering practical uncertainty sources. This relevant outcome is of utmost interest to practitioners, stakeholders, and regulators as it enables assessing alternative coordination schemes that may lead to economic losses, reduced reliability, and a suboptimal use of resources. Moreover, the resulting expansion decisions can be deemed as a reference investment plan constituting the basis for future developments under different coordination strategies.

The proposed methodology has been successfully validated using two test systems. Numerical results reveal that incorporating DG decisions gives rise to a substantial reduction in the total cost over the case with no DG. Additionally, the economic benefits with respect to a practical sequential approach have been illustrated. Moreover, compared to an alternative integrated planning model relying on the use of second-order cone programming for the distribution network, the effective performance of the proposed approach in terms of solution quality and computational effort is also empirically evidenced. Finally, results also show the convenience of using a stochastic approach as well as the suitability of the selected number of scenarios by exploring the trade-off between accuracy and computational tractability.

Further work will be devoted to implementing alternative coordination schemes and considering strategic planners, which may require the use of game theory while accounting for information confidentiality. Research will also be conducted to adopt a multistage or dynamic framework. Another interesting avenue of research is the extension of the proposed approach to consider practical aspects such as a more accurate power flow model, the discrete nature of generation investments, other generation technologies, and storage devices.

References

[1] L. Castanheira, G. Ault, M. Cardoso, J. McDonald, J. B. Gouveia, and Z. Vale, "Coordination of transmission and distribution planning and operations to maximise efficiency in future power systems," presented at the Int. Conf. Future Power Syst., Amsterdam, The Netherlands, Nov. 2005.

[2] R. Hemmati, R.-A. Hooshmand, and A. Khodabakhshian, "Comprehensive review of generation and transmission expansion planning," *IET Gener. Transm. Distrib.*, vol. 7, no. 9, pp. 955–964, Sep. 2013.

[3] P. S. Georgilakis and N. D. Hatziargyriou, "A review of power distribution planning in the modern power systems era: Models, methods and future research," *Electr. Power Syst. Res.*, vol. 121, pp. 89–100, Apr. 2015.

[4] Government of Spain. (Apr. 9, 2005). *Criterios de Desarrollo de la Red de Transporte*. [Online]. Available: https://boe.es/boe/dias/2005/04/09/pdfs/A12351-12358.pdf

[5] R. de Dios, F. Soto, and A. J. Conejo, "Planning to expand?" *IEEE Power Energy Mag.*, vol. 5, no. 5, pp. 64–70, Sep./Oct. 2007.

[6] *General Guidelines for Reinforcing the Cooperation between TSOs and DSOs*, European Federation of Local Energy Companies, Brussels, Belgium, 2015. [Online]. Available: http://cedec.com/files/default/entsoe-pp-tso-dso-web.pdf

[7] *Towards Smarter Grids: Developing TSO and DSO Roles and Interactions for the Benefit of Consumers*, European Network of Transmission System Operators for Electricity, Brussels, Belgium, 2015. [Online]. Available: https://docstore.entsoe.eu/Documents/Publications/Position%20papers%20and%20reports/150303_ENTSO-E_Position_Paper_TSO-DSO_interaction.pdf

[8] M. Caramanis, E. Ntakou, W. W. Hogan, A. Chakrabortty, and J. Schoene, "Co-optimization of power and reserves in dynamic T&D power markets with nondispatchable renewable generation and distributed energy resources," *Proc. IEEE*, vol. 104, no. 4, pp. 807–836, Apr. 2016.

[9] Z. Yuan and M. R. Hesamzadeh, "Hierarchical coordination of TSO-DSO economic dispatch considering large-scale integration of distributed energy resources," *Appl. Energy*, vol. 195, pp. 600–615, Jun. 2017.

[10] A. Papavasiliou and I. Mezghani, "Coordination schemes for the integration of transmission and distribution system operations," presented at the 20th Power Syst. Comput. Conf., Dublin, Ireland, Jun. 2018.

[11] M. Bragin, Y. Dvorkin, and A. Darvishi, "Toward coordinated transmission and distribution operations," presented at the 2018 IEEE PES Gen. Meeting, Portland, OR, USA, Aug. 2018.

[12] H. Le Cadre, I. Mezghani, and A. Papavasiliou, "A game-theoretic analysis of transmission-distribution system operator coordination," *Eur. J. Oper. Res.*, vol. 274, no. 1, pp. 317–339, Apr. 2019.

[13] I. Mezghani and A. Papavasiliou, "A mixed integer second order cone program for transmission-distribution system co-optimization," presented at the 2019 IEEE PowerTech, Milano, Italy, Jun. 2019.

[14] A. Nawaz, H. Wang, Q. Wu, and M. K. Ochani, "TSO and DSO with large-scale distributed energy resources: A security constrained unit commitment coordinated solution," *Int. Trans. Electr. Energy Syst.*, vol. 30, no. 3, Mar. 2020, Art. no. e12233.

[15] A. G. Givisiez, K. Petrou, and L. F. Ochoa, "A review on TSO-DSO coordination models and solution techniques," *Electr. Power Syst. Res.*, vol. 189, Dec. 2020, Art. no. 106659.

[16] T. Akbari and S. Z. Moghaddam, "Coordinated scheme for expansion planning of distribution networks: A bilevel game approach," *IET Gener. Transm. Distrib.*, vol. 14, no. 14, pp. 2839–2846, Jul. 2020.

[17] J. Liu, P. P. Zeng, H. Xing, Y. Li, and Q. Wu, "Hierarchical duality-based planning of transmission networks coordinating active distribution network operation," *Energy*, vol. 213, Dec. 2020, Art. no. 118488.

[18] H. K. Rad and Z. Moravej, "An approach for simultaneous distribution, sub-transmission, and transmission networks expansion planning," *Int. J. Electr. Power Energy Syst.*, vol. 91, pp. 166–182, Oct. 2017.

[19] J. Liu, H. Cheng, P. Zeng, L. Yao, C. Shang, and Y. Tian, "Decentralized stochastic optimization based planning of integrated transmission and distribution networks with distributed generation penetration," *Appl. Energy*, vol. 220, pp. 800–813, Jun. 2018.

[20] U. P. Müller *et al.*, "Integrated techno-economic power system planning of transmission and distribution grids," *Energies*, vol. 12, no. 11, Jun. 2019, Art. no. 2091.
[21] A. Nikoobakht, J. Aghaei, H. R. Massrur, and R. Hemmati, "Decentralised hybrid robust/stochastic expansion planning in coordinated transmission and active distribution networks for hosting large-scale wind energy," *IET Gener. Transm. Distrib.*, vol. 14, no. 5, pp. 797–807, Mar. 2020.
[22] J. R. Birge and F. Louveaux, *Introduction to Stochastic Programming*, 2nd ed. New York, NY, USA: Springer, 2011.
[23] D. Arthur and S. Vassilvitskii, "k-means++: The advantages of careful seeding," in *Proc. 18th Annu. ACM-SIAM Symp. Discret. Alg.*, 2007, pp. 1027–1035.
[24] G. L. Nemhauser and L. A. Wolsey, *Integer and Combinatorial Optimization*. New York, NY, USA: Wiley-Intersci., 1999.
[25] (2021). *IBM ILOG CPLEX*. [Online]. Available: https://www.ibm.com/analytics/cplex-optimizer
[26] R. Moreno, A. Street, J. M. Arroyo, and P. Mancarella, "Planning low-carbon electricity systems under uncertainty considering operational flexibility and smart grid technologies," *Philos. Trans. R. Soc. A-Math. Phys. Eng. Sci.*, vol. 375, Aug. 2017, Art. no. 20160305.
[27] L. Baringo and A. J. Conejo, "Transmission and wind power investment," *IEEE Trans. Power Syst.*, vol. 27, no. 2, pp. 885–893, May 2012.
[28] Y. Wang, S. Liu, J. Wang, and B. Zeng, "Capacity expansion of wind power in a market environment with topology control," *IEEE Trans. Sustain. Energy*, vol. 10, no. 4, pp. 1834–1843, Oct. 2019.
[29] S. Binato, M. V. F. Pereira, and S. Granville, "A new Benders decomposition approach to solve power transmission network design problems," *IEEE Trans. Power Syst.*, vol. 16, no. 2, pp. 235–240, May 2001.
[30] D. K. Molzahn *et al.*, "A survey of distributed optimization and control algorithms for electric power systems," *IEEE Trans. Smart Grid*, vol. 8, no. 6, pp. 2941–2962, Nov. 2017.
[31] Z. Li, W. Wu, B. Zhang, and X. Tai, "Analytical reliability assessment method for complex distribution networks considering post-fault network reconfiguration," *IEEE Trans. Power Syst.*, vol. 35, no. 2, pp. 1457–1467, Mar. 2020.
[32] R. A. Jabr, "Radial distribution load flow using conic programming," *IEEE Trans. Power Syst.*, vol. 21, no. 3, pp. 1458–1459, Aug. 2006.
[33] J. F. Franco, M. J. Rider, and R. Romero, "A mixed-integer quadratically-constrained programming model for the distribution system expansion planning," *Int. J. Electr. Power Energy Syst.*, vol. 62, pp. 265–272, Nov. 2014.
[34] G. Muñoz-Delgado, J. Contreras, J. M. Arroyo, A. Sanchez de la Nieta, and M. Gibescu. *Integrated Transmission and Distribution System Expansion Planning under Uncertainty: Test Data and Results*. Accessed: Mar. 2, 2021. [Online]. Available: https://ieee-dataport.org/documents/integrated-transmission-and-distribution-system-expansion-planning-under-uncertainty-test
[35] R. Mínguez and R. García-Bertrand, "Robust transmission network expansion planning in energy systems: Improving computational performance," *Eur. J. Oper. Res.*, vol. 248, no. 1, pp. 21–32, Jan. 2016.
[36] G. Muñoz-Delgado, J. Contreras, and J. M. Arroyo, "Distribution network expansion planning with an explicit formulation for reliability assessment," *IEEE Trans. Power Syst.*, vol. 33, no. 3, pp. 2583–2596, May 2018.
[37] (2021). *GAMS Development Corporation*. [Online]. Available: http://www.gams.com
[38] (2021). *Gurobi Optimization*. [Online]. Available: https://www.gurobi.com
[39] L. L. Garver, "Transmission network estimation using linear programming," *IEEE Trans. Power App. Syst.*, vol. PAS-89, no. 7, pp. 1688–1697, Sep./Oct. 1970.
[40] (2021). *@RISK*. [Online]. Available: https://www.palisade.com/risk
[41] (2021). *IEEE 118-Bus System*. [Online]. Available: http://motor.ece.iit.edu/data/
[42] M. E. Samper and A. Vargas, "Investment decisions in distribution networks under uncertainty with distributed generation—Part II: Implementation and results," *IEEE Trans. Power Syst.*, vol. 28, no. 3, pp. 2341–2351, Aug. 2013.

Gregorio Muñoz-Delgado (Member, IEEE) received the Ingeniero Industrial, M.Sc., and Ph.D. degrees from the Universidad de Castilla-La Mancha, Ciudad Real, Spain, in 2012, 2013, and 2017, respectively.

He is currently an Associate Professor with the Universidad de Castilla-La Mancha. His research interests are in the fields of power systems planning, operation, and economics.

Javier Contreras (Fellow, IEEE) received the B.S. degree in electrical engineering from the University of Zaragoza, Zaragoza, Spain, in 1989, the M.Sc. degree from the University of Southern California, Los Angeles, CA, USA, in 1992, and the Ph.D. degree from the University of California at Berkeley, Berkeley, CA, USA, in 1997.

He is a Professor with the Universidad de Castilla-La Mancha, Ciudad Real, Spain. His research interests include power systems planning, operation, economics, as well as electricity markets.

José M. Arroyo (Fellow, IEEE) received the Ingeniero Industrial degree from the Universidad de Málaga, Málaga, Spain, in 1995, and the Ph.D. degree from the Universidad de Castilla-La Mancha, Ciudad Real, Spain, in 2000.

He is currently a Full Professor of Electrical Engineering with the Universidad de Castilla-La Mancha. His research interests include operation, planning, and economics of power systems, as well as optimization.

Agustin Sanchez de la Nieta (Member, IEEE) received the B.S. and Ph.D. degrees in industrial engineering from the Universidad de Castilla-La Mancha, Ciudad Real, Spain, in 2008 and 2013, respectively.

He is currently a Postdoctoral Fellow with the Copernicus Institute of Sustainable Development, Faculty of Geosciences, Utrecht University, Utrecht, The Netherlands. His research interests include power systems planning and economics, electricity markets, forecasting, and risk management for renewable energy sources.

Madeleine Gibescu (Member, IEEE) received the Dipl.Eng. degree in power engineering from University Politehnica, Bucharest, Romania, in 1993, and the M.Sc. and Ph.D. degrees in electrical engineering from the University of Washington, Seattle, WA, USA, in 1995 and 2003, respectively.

She is currently a Full Professor of Integration of Intermittent Renewable Energy with the Copernicus Institute of Sustainable Development, Faculty of Geosciences, Utrecht University, Utrecht, The Netherlands. Her research interests are in the area of smart and sustainable power systems.